Altgen, Michael; Uimonen, Tuuli; Rautkari, Lauri

The effect of de- and re-polymerization during heat-treatment on the mechanical behavior of Scots pine sapwood under quasi-static load

Published in:
Polymer Degradation and Stability

DOI:
10.1016/j.polymdegradstab.2017.12.007

Published: 01/01/2018

Document Version
Peer-reviewed accepted author manuscript, also known as Final accepted manuscript or Post-print

The effect of de- and re-polymerization during heat-treatment on the mechanical behavior of Scots pine sapwood under quasi-static load

Michael Altgen[1*], Tuuli Uimonen[1], Lauri Rautkari[1]

[1] Department of Bioproducts and Biosystems, School of Chemical Engineering, Aalto University, Vuorimiehentie 1, 02150 Espoo, Finland

[*]corresponding author: michael.altgen@aalto.fi; phone: +358503841611

Abstract

Loss in strength and ductility is a major drawback for the heat-treatment of solid wood. Previous studies focused mainly on the de-polymerization of cell wall constituents as a cause and the importance of the preferential removal of hemicelluloses. This study tested the hypothesis that the mechanical behavior of wood is additionally affected by re-polymerization reactions within the cell wall matrix during heat-treatment. This was achieved by comparing changes in chemical composition, FT-IR spectra, and mechanical properties of Scots pine sapwood that was heat-treated in either dry state in superheated steam or in wet state using pressurized hot water. Although preferential de-polymerization of hemicelluloses was evident for both heat-treatment techniques, the analysis of the chemical composition and FT-IR spectroscopy indicated additional re-polymerization reactions within the cell wall matrix of dry heat-treated wood. The consequent formation of covalent bonds and cross-links increased the resistance against compression loads and hindered inelastic deformation during bending. This resulted in an additional reduction in bending strength and strain energy density of dry compared to wet heat-treated wood. Re-polymerization reactions during heat-treatments of wood in dry state were suggested as the main cause for the brittle failure under bending loads, while the effect of hemicellulose-removal on brittleness was much smaller than stated previously.

Keywords: Chemical composition; Mechanical properties; FT-IR spectroscopy; Scanning electron microscopy; Thermal modification; Wood

1. Introduction

When exposed to heat, various chemical reactions take place that change the chemical composition and the structural arrangement of the wood cell wall. Chemical changes caused by heat-exposure are induced intentionally during heat-treatment (HT) of solid wood on industrial-scale. Various industrial HT processes are operated in Europe, which are reviewed in detail by Militz and Altgen [1]. During most HT processes for solid wood, e.g. the ThermoWood® process that has the largest market shares of heat-treated wood produced in Europe [2], temperatures between 160 and 240 °C are applied for several hours to nearly dry wood material. This enables the use of European wood species in exterior applications [1]. However, HT is a balance between improving the dimensional stability [3] and the resistance to decay fungi [4,5] of wood on the one hand, while reducing its strength and ductility on the other hand [6–9]. The latter causes problems in load-bearing applications, and can also be the result of heat-induced chemical changes during re-drying of fire-retardant-treated wood [10], or hot-pressing of wood composites [11]. Despite the many investigations dealing with the change in the macro-scale mechanical properties of wood by heat-exposure [6,8], the underlying modes of action remain a subject for research.

Mechanical behavior of heat-treated wood is often determined in quasi-static three-point bending [7,12–14]. Stresses developed in three-point bending are a combination of compression stresses in the material at the top of the sample and tensile stresses in the material at the opposite region, while shear stresses develop in the neutral zone, where bending stresses become zero. When testing small clear samples of unmodified wood, the tensile strength usually exceeds the compression strength, thus bending is governed by compression behavior with pronounced inelastic deformation [15]. The effect of HT on the bending behavior of wood is most noticeable as a loss in strain energy (area below the stress-strain curve) caused by a reduction in strength and ductility, while the stiffness remains almost unchanged. The extent of this change in the mechanical behavior is dependent on the treatment temperature and duration applied [7,9,14], and is predominantly caused by the chemical changes occurring in the wood cell wall during HT [9].

There is a complex link between the chemical composition as well as the ultra-structural arrangement of the cell wall and the mechanical behavior of wood under various loads [16–18]. When an external load is applied, the cell wall polymers contribute in different degrees to the strength, stiffness and ductility of the wood. Cellulose microfibrils act as tensile reinforcements. They exhibit an extremely high modulus of elasticity (MOE) under tension and contribute greatly to the stiffness of the cell wall [19]. Under compression, however, cellulose microfibrils buckle easily [20]. This low resistance against compression loads is compensated by the cell wall matrix that contains a rigid lignin network [20–22]. Lignin also limits the access of water to the cell wall, enabling it to retain its strength and stiffness in humid environments [23,24]. However, lignin is not bonded to the cellulose directly, thus hemicelluloses are required as coupling agents that enable the transfer of stresses between the individual polymers, so that the cell wall acts as a continuum. Although hemicelluloses are presumably not bonded to the cellulose microfibrils covalently either, hydrogen bonds between these polymers are formed, which is further supported by physical entanglement within the non-crystalline regions of the microfibrils [17,25,26]. Hemicelluloses are covalently bonded to the lignin by ester, ether and glyosidic bonds to form lignin carbohydrate complexes (LCC) that are difficult to separate [25].

During exposure of wood to elevated temperatures by HT, many chemical reactions of the cell wall polymers take place, which result in a deviation from the chemical composition and ultra-structural arrangement of untreated wood. Amorphous hemicelluloses are much more sensitive to thermal degradation than the semi-crystalline cellulose or the lignin [27]. Hemicelluloses are hydrolyzed, resulting in shorter polymer chains, and subsequent dehydration leads to the formation of furan-type intermediates, such as furfural and hydroxyl methyl furfural (HMF) derived from pentoses and hexoses, respectively [28,29]. Furfural and HMF become volatile at elevated temperatures and are released from the wood to cause a mass loss (ML) [30].

The change in bending properties as a consequence of HT can often be described as a function of ML [31,32], which might be interpreted as evidence that the change in the mechanical behavior

is pre-dominantly caused by the de-polymerization of hemicelluloses. Removing the hemicelluloses by HT is believed to affect the load sharing capability of the cell wall, thus internal stresses in wood caused by an external load are no longer distributed over the cell wall polymers as a continuum [6]. As recently reviewed by Winandy [8], a vast number of studies on the effects of elevated temperature, chemical treatments or biological decay point towards a singular relationship between strength loss and a uniform degradation sequence of the cell wall polymers, i.e. the hemicelluloses. Winandy [8] hypothesized that strength loss during heat-exposure proceeds in the order of: (1) hydrolytic de-polymerization of side-chain hemicelluloses, which is followed by (2) the hydrolytic de-polymerization of the main-chain hemicelluloses, and finally, at high strength loss levels by (3) the de-polymerization of cellulose and/or lignin.

However, this hypothesis does not consider the many re-polymerization reactions and ultra-structural rearrangements that occur in addition to the de-polymerization of the cell wall polymers [33]. During HT of wood, re-polymerization by ester bond formation [34,35], or by condensation reactions involving lignin and furan-type intermediates derived from hemicelluloses degradation [33,36,37], are likely pathways for modification of the cell wall matrix ultra-structure. Such covalent bond formation by re-polymerization is likely to affect the mechanical performance of heat-treated wood. Unfortunately, this effect is often overlooked, because it is difficult to separate the effects of cell wall polymer de- and re-polymerization during HT, as they are interrelated and occur simultaneously.

We hypothesized that re-polymerization reactions contribute significantly to the decrease in strength and ductility by HT. To test this hypothesis we compared the effect of HT of wood in dry state at high temperatures (180-240 °C) in a superheated steam atmosphere with HT of wood in wet state at mild temperatures (120-170 °C) in pressurized hot water. By variation of the treatment temperature for both HT techniques, we aimed at a wide range of thermal degradation intensities, which was quantified by ML. We speculated that the HT of wood in wet state favors de-polymerization over re-polymerization reactions compared to HT of dry wood at high

temperatures. We analyzed this shift in de- and re-polymerization reactions by FT-IR spectroscopy and the analysis of the chemical composition and compared its impact on the change in the mechanical performance under quasi-static load. Since the treatment conditions applied differed significantly between the HT techniques, the results were analyzed as a function of ML.

2. Material and methods

2.1. Material

Kiln-dried boards of Scots pine (*Pinus sylvestris* L.) wood were used for all experiments. For bending tests, samples with dimensions of 13×13×180 mm^3 (r×t×l) with 15 replicates per variety (treatment process, peak temperature) were heat treated, while for compression tests samples with dimensions of 23×23×110 mm^3 (r×t×l) with six replicates per variety were treated. The samples were clear of heartwood, knots and visible defects. All samples were oven-dried prior to HT using a temperature sequence of 40, 60, 80 and finally 103 °C, with each temperature held for ca. 24 h, before the determination of initial dry mass.

2.2. Heat treatments

Wet heat-treatment (HT_{wet}): The samples were vacuum-impregnated (ca. 50 mbar for 1 h) with deionized water 24 hours before HT_{wet}. HT_{wet} was conducted in an air bath digester, which held several autoclaves (2.5 l volume) that were heated in hot air while rotating slowly. The samples were placed in the autoclaves together with deionized water in a solid to liquid ratio of 1:20 (g/g). The water temperature was increased fast until reaching 80 °C and then at a constant rate of 55 °C h^{-1} until reaching the respective peak temperature: 120, 130, 140, 150, 160 or 170 °C. After a 120 min. holding stage at the respective peak temperature, the vessels were removed from the hot air bath and placed in a cold water bath for 30 min under continuous water flow. Finally, any remaining pressure was released via a needle valve and the samples were removed from the vessels.

Dry heat-treatment (HT_{dry}): The samples were kept in dry state in a desiccator with silica gel until HT_{dry}. HT_{dry} was performed in an oven with continuous insertion of superheated steam. An initial temperature of 105 °C was applied for 30 min and then the temperature was increased stepwise by 15 °C every 30 min until reaching the respective peak temperature: 180, 195, 210, 225 or 240 °C, which was held for 180 min. After that, the oven heating was switched off and the temperature decreased to <100 °C within one hour, after which the samples were removed from the oven.

All samples, including the reference samples, were leached with deionized water after the treatment. Dry heat-treated and reference samples were vacuum-impregnated with deionized water before leaching. Within the course of two weeks, the water was changed daily, before the samples were dried carefully at ambient conditions for a minimum of one week and then in an oven by applying the temperature sequence described above. Besides removal of remaining, water-soluble degradation products, the water-leaching caused maximum swelling of the samples to remove any reversible, drying related-effects [13,38]. The mass loss caused by treatment and leaching, ML (%), was calculated based on the dry mass of each sample before and after the process.

2.3. Chemical composition

Samples tested in three-point bending (2.5) were milled and mixed in a Wiley mill to pass through a 30 mesh screen. 6 g of wood particles were extracted in a Soxhlet apparatus with acetone for 6 h. Determination of carbohydrates and lignin was performed on the extracted samples according to the analytical procedure (NREL/TP-510-42618) issued by the U.S. National Renewable Energy Laboratory [39]. Carbohydrates were determined by High Performance Anion Exchange Chromatography with Pulse Amperometric Detection (HPAEC-PAD) in a Dionex ICS-3000 column. The acid-soluble lignin was determined in a Shimadzu UV-2550 spectrophotometer using a wavelength of 205 nm and an absorptivity constant of 110 L g^{-1} cm^{-1}. The acid-insoluble fraction was determined gravimetrically after drying at 103 °C for 12 h. The lignin percentage

was calculated as the sum of the acid-soluble and the acid-insoluble fraction. All samples were analyzed in duplicate. The results are given as ratios with the value of the unmodified reference set to 1.

2.4. FT-IR spectroscopy

FT-IR spectra were collected using a Bio-Rad FTS-6000 spectrometer (Cambridge, MA, USA) with a MTEC 300 photoacoustic detector (Ames, IA, USA) using a 10 kHz mirror velocity and a resolution of 8 cm^{-1}. First, the background spectrum with standard carbon black was measured. Then, the same acetone-extracted wood particles as in 2.3 were measured after drying at 103 °C for 12 h and cooling in a desiccator with silica gel. A small amount of particles was put into a detection cell, which was placed into the detector. The cell was flushed with helium gas for 5 min before the cell was sealed and the spectrum was recorded. For each measurement, 400 scans per spectrum were collected and processed with the WIN-IR Pro 3.4 software (Digilab, Randolph, MA, USA). The measurements were done in triplicate and all spectra were baseline corrected, but not normalized. Average spectra of these measurements are presented, focusing on the region between 1850 and 800 cm^{-1}. Additionally, the absorbance ratio ($A_{1724\text{-}1736}/A_{2900}$) was calculated by relating the maximum absorbance in the region between 1724 and 1736 cm^{-1} to the maximum absorbance at ca 2900 cm^{-1}.

2.5. Mechanical testing

All samples were conditioned at 20 °C and 65 % RH after final drying until the change in mass was less than 0.1 % 24 h^{-1} and then planed and cut to dimensions of 10×10×180 mm^3 and 20×20×30 mm^3 (r×t×l) for bending and compression samples, respectively. The sample dimensions were determined in conditioned state before testing.

The three-point bending test was conducted with 15 replicates per sample group on a universal testing machine (Zwick 1475) equipped with a 20 kN load cell and combined with a MTS Premium Elite controller. The span length was set to 150 mm and the load was applied in the tangential direction at a rate of 3 mm min^{-1}. Deflection (δ, in mm) was set to zero at a load (P, in

N) of ca. 4 N. P and δ were converted into stress (Ϭ, in N mm^{-2}) and strain (Ɛ, in mm mm^{-1}), respectively, by applying the following equations:

$$\sigma = (3\ P\ L)/(2\ b_0\ h_0^2), \quad (1)$$

$$\varepsilon = (6\ \delta\ h)/L^2, \quad (2)$$

where L is the span length (150 mm), b_0 and h_0 are the width (mm) and the height (mm) of the samples before testing, respectively. Bending strength (MOR, in N mm^{-2}) was defined as the maximum stress. Modulus of elasticity (MOE, in N mm^{-2}) was determined as the slope of a linear regression curve of the stress-strain curve within the range between 10 and 40 % of MOR. Strain energy density (u, in kJ mm^{-3}) was computed as the area below the stress-strain curve up to the strain at maximum stress ($Ɛ_{max}$; in mm mm^{-1}), according to equation (3):

$$u = \int_0^{\varepsilon_{max}} \sigma\ d\varepsilon \quad (3)$$

$Ɛ_{max}$ and u were divided into their elastic (potential energy) and inelastic (dissipated energy) proportions as shown in **Figure 1**. Elastic strain ($Ɛ_{elastic}$) and elastic strain energy density ($u_{elastic}$) were calculated according to equations 4 and 5.

$$\varepsilon_{elastic} = MOR/MOE \quad (4)$$

$$u_{elastic} = MOR \times (\varepsilon_{elastic}/2) \quad (5)$$

Brittleness was quantified by the brittleness index (BI, in %) as described by Zou et al. [40] for tensile tests on papers, according to equation (6):

$$BI = 100 \times (u_{elastic}/u) \quad (6)$$

A high BI characterizes a material that absorbs very little energy by inelastic deformation until reaching maximum stress.

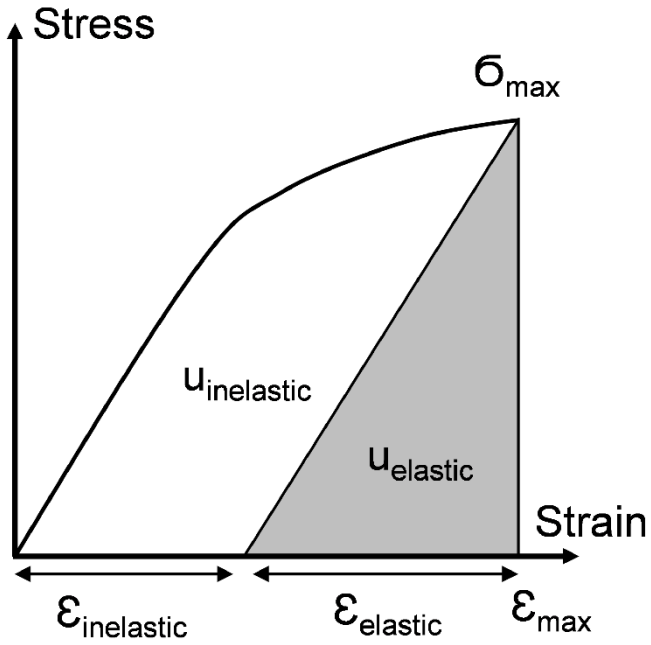

Figure 1: Schematic stress-strain curve showing MOR (σ_{max}), strain at maximum stress (ε_{max}), elastic ($\varepsilon_{elastic}$) and inelastic strain ($\varepsilon_{inelastic}$), as well as elastic ($u_{elastic}$) and inelastic strain energy density ($u_{inelastic}$).

The compression test parallel to the grain was conducted with 18 replicates per sample group on the same universal testing machine, but with a 100 kN load cell. The load was applied in the longitudinal direction at a rate of 1 mm min^{-1}. Displacement (in mm) was set to zero at a load (P, in N) of ca. 30 N. Stress (N mm^{-2}) was calculated by relating P to the cross-sectional area before testing (in mm^2) and maximum stress was defined as compression strength (CS).

After completion of the bending and compression tests, the dry mass of the samples was determined after oven-drying at 103°C to calculate the specific gravity (in kg mm^{-3}) by relating the volume in conditioned state to the respective dry mass. By dividing MOR, MOE, u and CS by the specific gravity, the specific MOR (MOR_{spec}; in N mm kg^{-1}), the specific MOE (MOE_{spec}; in N mm kg^{-1}), the specific strain energy density (u_{spec} in kJ kg^{-1}) and the specific CS (CS_{spec}, in N mm kg^{-1}) were computed for each sample. MOR_{spec}, MOE_{spec}, u_{spec} and CS_{spec} are given as ratios with the value of the unmodified reference set to 1.

2.6. SEM observations

Samples with bending properties close to the group average were selected for the investigation of the fracture surface by scanning electron microscopy (SEM). Samples treated by HT_{dry} at 240 °C and samples treated by HT_{wet} at 170 °C, with bending properties close the group average were selected for the investigation of the fracture surface by scanning electron microscopy (SEM). Small cross-cuts with a length of ca. 40 mm were taken from the bending samples for SEM observations. The samples were dried at 50 °C and <100 mbar for 24 h and sputter-coated with gold-palladium, before the observation in a Zeiss Sigma VP SEM (Oberkochen, Germany). The observation was limited to the tension side of the fracture surface.

3. Results and discussion

3.1. Chemical composition

The changes in chemical composition support our hypothesis of preferential de-polymerization during HT_{wet} and additional re-polymerization during HT_{dry}. However, the general trend of a decreased percentage of hemicellulose sugars, while the percentage of glucose (mostly originating from the cellulose) and the percentage of lignin increase, was evident for HT_{wet} and HT_{dry}, as can be seen in **Figure 2** and **Table 1**. It is a result of the preferential de-polymerization of the amorphous hemicelluloses during HT, which causes the accumulation of cellulose and lignin. The presence of water compensated for the lower treatment temperatures and shorter treatment durations during HT_{wet}, due to the catalytic effect of hydronium ions created by water auto-ionization on de-polymerization reactions. The presence of water also facilitated the formation of acetic acid by cleavage of acetyl groups from the hemicelluloses, which contributed further to the catalytic effect of water [41,42]. As a result, the ML range was larger for HT_{wet} (max. 25.2 %) than for HT_{dry} (max. 14.1 %), even though the treatment temperatures and durations applied were much lower for HT_{wet}. However, the rate at which the chemical composition changed as a function of ML differed notably between the two process techniques, which can be explained by differences in the ratio of de-polymerization to re-polymerization reactions.

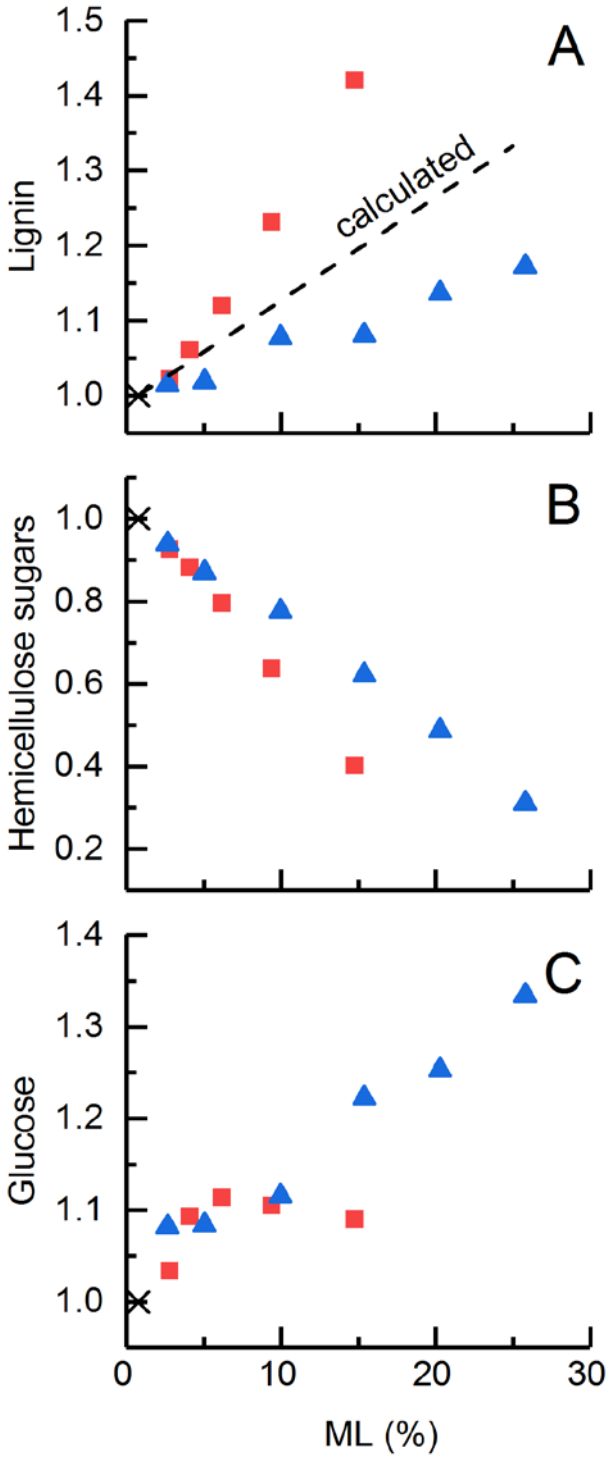

Figure 2: Changes in chemical composition given as ratios in dependence on the mass loss during the process (ML, %, N=15) for unmodified (cross), dry heat-treated (squares) and wet heat-treated (triangles) Scots pine sapwood. A) Lignin ratio, with the dashed line marking the lignin percentage that is calculated from the reference value based on the assumption that the mass loss is purely based on carbohydrate removal; B) hemicellulose sugar ratio based on all sugars detected except glucose; C) glucose ratio

The increase in lignin percentage as a function of ML (**Figure 2** A**)** was larger after HT_{dry} than after HT_{wet}. The increase can also be compared with the calculated increase in lignin percentage, which is based on the lignin percentage of the unmodified reference and the assumption that the ML is purely based on the removal of carbohydrates. After HT_{dry}, the increase in lignin percentage was larger than calculated, which coincides with the study by Inari et al. [36]. Furan-type derivatives, such as furfural and HMF derived from the dehydration of sugars, have been suggested to be involved in condensation and cross-linking reactions with lignin in previous studies [33,36,37]. These degradation products may add to the increase in lignin percentage that is based on hemicellulose removal. Such formation of additional covalent bonds results in a modified, more cross-linked lignin carbohydrate complex (LCC) within the cell wall matrix [33]. Furthermore, carbonium ions formed by de-polymerization of ether linkages within the lignin are involved in re-polymerization reactions that form stable carbon-carbon linkages at sufficiently high temperatures. These carbon-carbon linkages increase the lignin's resistance against further de-polymerization [43,44].

In contrast, HT_{wet} lead to a lower increase in lignin percentage than calculated. It indicates that the reaction rates for de-polymerization of bonds within the lignin outweighed the reaction rates for re-polymerization at low temperatures and aqueous conditions, in line with the results of Borrega et al. [44]. The presence of water not only facilitates de-polymerization by hydrolytic cleavage of acetyl groups on hemicelluloses or glycosidic linkages in polysaccharides, but also the cleavage of ether linkages within the lignin [41,43]. Re-polymerization by condensation reactions involving carbonium ions formed by cleavage of ether linkages in lignin are more prominent at temperatures exceeding 200 °C, but are not suppressed in aqueous conditions [43,44]. However, there is evidence that the dehydration of sugars to furfural or HMF is less facile in the presence of water, resulting in fewer reactants for re-polymerization. In studies on the hydrolysis of carbohydrates in ionic liquids, it was shown that elevated percentages of water during the treatments increase the monosaccharide yield, but gradually reduce their dehydration

to furan-type intermediates (furfural/HMF) and the subsequent formation of humins by condensation reactions involving these intermediates [45–47]. This water-related effect was first explained by a shift in the chemical reactions according to Le Chatelier's principle [45]. Later, it was suggested that water molecules compete with the hydroxyl groups on glucose and xylose (and possibly on other monosaccharides as well) for available protons, which hinders protonation of glucose or xylose that initiates their dehydration to HMF or furfural, respectively [46,47]. Probably, the same effect is evident during HT_{wet} of solid wood, resulting in fewer re-polymerization reactions compared to HT_{dry}.

Table 1: Composition of sugars (%) measured for the bending samples. Ratios with the respective reference value set to 1 are given in parenthesis.

Variety	Glucose (%)	Mannose (%)	Xylose (%)	Galactose (%)	Arabinose (%)	Rhamnose (%)
Ref[a]	41.2 (1)	11.5 (1)	5.1 (1)	4.5 (1)	1.5 (1)	0.2 (1)
HT_{dry}						
180°C	42.6 (1.0)	12.0 (1.0)	5.3 (1.0)	2.5 (0.6)	1.2 (0.8)	0.1 (0.8)
195°C	45.1 (1.1)	12.4 (1.1)	4.7 (0.9)	2.0 (0.5)	0.8 (0.5)	0.1 (0.5)
210°C	45.9 (1.1)	11.8 (1.0)	3.9 (0.8)	1.8 (0.4)	0.5 (0.3)	0.1 (0.4)
225°C	45.5 (1.1)	10.3 (0.9)	2.7 (0.5)	1.2 (0.3)	0.3 (0.2)	ND
240°C	44.9 (1.1)	6.7 (0.6)	1.7 (0.3)	0.6 (0.1)	0.1 (0.1)	ND
HT_{wet}						
120°C	44.6 (1.1)	12.4 (1.1)	5.2 (1.0)	2.8 (0.6)	0.9 (0.6)	TR[b]
130°C	44.7 (1.1)	11.7 (1.0)	4.7 (0.9)	2.8 (0.6)	0.4 (0.3)	0.1 (0.4)
140°C	46.0 (1.1)	10.3 (0.9)	4.8 (0.9)	2.3 (0.5)	0.2 (0.2)	0.1 (0.3)
150°C	50.4 (1.2)	9.0 (0.8)	3.9 (0.8)	1.1 (0.3)	0.1 (0.03)	ND[c]
160°C	51.6 (1.3)	6.4 (0.6)	3.7 (0.7)	0.9 (0.2)	0.1 (0.04)	ND[c]
170°C	55.0 (1.3)	3.5 (0.3)	3.3 (0.6)	0.3 (0.1)	ND	ND[c]

[a]Ref = Reference; [b]TR = traces found; [c]ND = not detected

Strong re-polymerization during HT_{dry} and preferential de-polymerization during HT_{wet} also affected the loss in sugars as a function of ML. The hemicellulose sugar ratio (sum of all detected sugars except glucose; **Figure 2** B) decreased stronger by HT_{dry} than by HT_{wet}. ML underestimated the actual de-polymerization of hemicelluloses by HT_{dry}, presumably because hemicellulose degradation products were partly fixed within the cell wall by re-polymerization reactions to add to the wood dry mass. In contrast, ML overestimated the de-polymerization of hemicelluloses during HT_{wet}, because the de-polymerization of the lignin caused additional ML. ML is obviously only a measure of the wood substance removed, but is insensitive to changes in

the structural arrangement within the solid residue. Therefore, differences in formation or cleavage of covalent bonds within the cell wall during HT_{dry} or HT_{wet} are not detected by ML, which needs to be considered during the interpretation of changes in mechanical properties as a function of ML.

The analysis of monosaccharides found in the wood hydrolysates (**Table 1**) is in line with the degradation sequence of wood under thermal or thermochemical conditions reviewed by Winandy [8]. Monosaccharides found primarily at the side chains (arabinose and galactose) were removed more rapidly by HT than monosaccharides that built the main chain of the hemicelluloses (mannose and xylose). It is also noticeable that while the glucose percentage increased monotonically by HT_{wet} (**Table 1**), it decreased after reaching a maximum for temperatures exceeding 210 °C during HT_{dry}. For the severest HT_{dry} (240 °C for 3 h), the glucose percentage as a function of ML was clearly lower than for wet heat-treated samples (**Figure 2** C). Although some glucose originates from the hemicellulose fraction, the glucose percentage should closely reflect the cellulose percentage. Thus, an increasing glucose ratio evidences cellulose accumulation, while a decrease in glucose indicates the start of cellulose degradation during HT_{dry}. Since the cellulose microfibrils are highly ordered, they are mostly inaccessible for water [48], which makes them very resistant against hydrolysis during HT_{wet} [49]. At temperatures exceeding 200 °C, however, thermal degradation of cellulose begins gradually, which starts at weak links and amorphous regions [50].

3.2. FT-IR spectroscopy

For heat-treated wood, the interpretation of FT-IR spectra is complicated by the various thermal degradation reactions that affect all wood polymers and make it difficult to select a peak that remains unaffected for the normalization of the spectra. Therefore, the spectra were not normalized and only qualitative differences caused by the HT techniques can be derived from **Figure 3**.

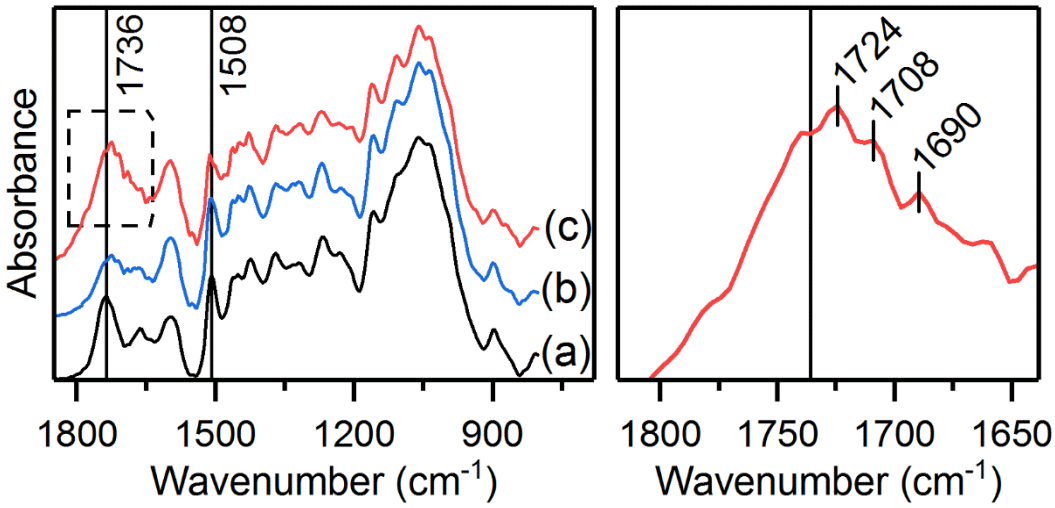

Figure 3: FT-IR spectra of unmodified wood (a), wood after HT_{wet} at 170 °C (b), and wood after HT_{dry} at 240 °C in the region between 1850 and 800 cm^{-1}. The spectra were shifted vertically for better visibility. The spectrum of dry heat-treated wood in the region between 1800 and 1630 cm^{-1} (dotted box) is shown in detail.

Small differences were evident at the peak around 1508 cm^{-1}, which can be assigned to aromatic skeletal vibrations in lignin [51]. HT caused a shift towards higher wavenumbers, which has previously been explained by the occurrence of condensation reactions within the lignin [51,52]. This shift was first evident after HT_{dry} at 195 °C and after HT_{wet} at 160 °C. However, differences between the HT techniques that could be related to condensation and cross-linking reactions involving furan-type intermediates formed from the hemicelluloses and lignin were not found. This is probably, because the absorbance by the aromatic rings of furan-type intermediates and lignin overlap.

Large differences were evident in the region between 1650 and 1750 cm^{-1}, which is characteristic for carbonyl stretching of ester and carboxyl groups in wood [51,53]. In unmodified wood, a maximum was found at 1736 cm^{-1} that was assigned to unconjugated carbonyl and ester bonds found mainly in wood hemicelluloses [51]. As reported previously [54], this maximum shifted to lower wavenumbers by HT, with a maximum at 1724 cm^{-1} for the highest treatment temperatures of HT_{dry} and HT_{wet}. This is in line with the formation of a peak at 1722 cm^{-1} during HT of pure hemicelluloses in a nitrogen atmosphere [35], as well as with the formation of a peak at 1720 cm^{-1} during HT of lignin in air [55], both evidencing the generation of carbonyl groups. Furthermore,

new peaks were also formed at 1708 and 1690 cm^{-1}, probably originating from unconjugated carbonyl and ester groups and from conjugated aldehydes and carboxylic acids, respectively [51].

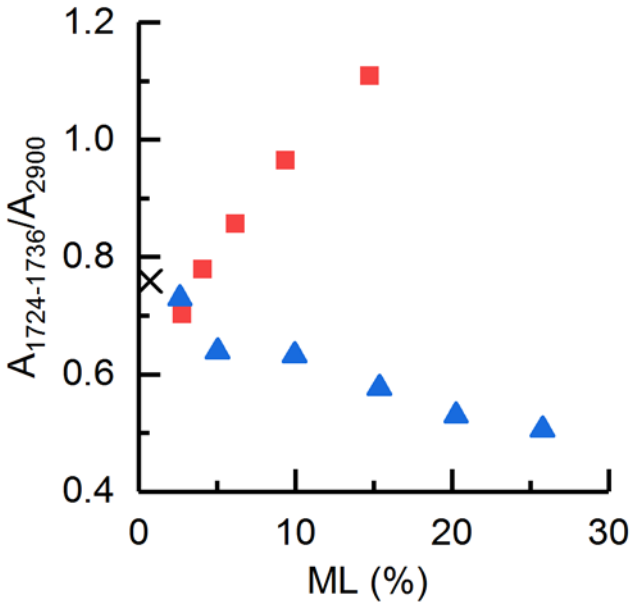

Figure 4: Ratio of the maximum absorbance between 1724 and 1736 cm^{-1} related to the absorbance at ca. 2900 cm^{-1} in dependence on the mass loss during the process for unmodified (cross), wet heat-treated (triangles) and dry heat-treated (squares) Scots pine sapwood.

To quantify differences between the HT techniques, the maximum absorbance in the range between 1724 and 1736 cm^{-1} was related to the maximum absorbance at ca. 2900 cm^{-1} (**Figure 4**). The peak at ca. 2900 cm^{-1} is characteristic for C-H stretching vibrations. Although a small decrease can be expected at this peak [54], it is less sensitive to HT effects than peaks associated with ester bonds, hydroxyl, carbonyl or methoxyl groups [56]. Furthermore, the change is less ambiguous compared to the aromatic skeletal vibration in lignin (1508 cm^{-1}), which can increase or decrease by HT depending on whether the increase in lignin percentage [52,54], or the aromatic ring opening in lignin [57] dominates. By HT_{wet}, the absorbance ratio decreased as a function of ML, in line with the hypothesis of (ester-) bond cleavage and hemicellulose de-polymerization dominating over bond formation in the presence of water. Cleavage of acetyl groups from the wood hemicelluloses, resulting in a decrease in absorbance at 1736 cm^{-1}, is an important step during wood auto-hydrolysis, as it results in the formation of acetic acid [41,42]. By HT_{dry}, the absorbance ratio increased as a function of ML after a small initial decrease at a ML of less than

5 %. This coincides with an increased absorbance between 1700 and 1730 cm^{-1} observed by Kotilainen [54] for dry heat-treated softwoods. It indicates that the formation of ester bonds and carbonyl groups in the wood dominates over de-polymerization and bond cleavage during HT_{dry}. Esterification reactions involving the carboxylic acids formed during HT and hydroxyl groups in wood [34], as well as the generation of new carboxyl groups in hemicelluloses and lignin during heat exposure are possible explanations for the increase in the absorption ratios [35,55]. Besides pyrolytic degradation reactions induced by elevated temperatures, residual air within the superheated steam atmosphere during HT_{dry} might contribute to the increase in absorbance ratio by catalyzing oxidative carboxylation [53,55]. Carboxyl groups and ester bonds may overlap in FT-IR spectra. However, the carboxyl groups formed are likely to react with hydroxyl groups of other wood polymers in acidic, dry heat conditions to form ester bonds, which would contribute to a more cross-linked cell wall matrix in dry heat-treated wood.

3.3. Mechanical behavior

All mechanical properties, except for the brittleness index, were computed as specific values by relating them to the respective specific gravity. Thereby, the direct effect of mass loss that results in the distribution of the stresses over less cell wall material was removed. The calculation as specific values also reduced the remaining impact of density variations in the raw material on the mechanical properties after HT. Therefore, changes in bending properties as a function of ML (**Figure 5**) can be directly assigned to changes in the chemical composition and/or to changes in the arrangement of the cell wall polymers.

The MOE_{spec} ratio (**Figure 5** A) remained nearly constant in the ML range up to 20 % and only a slight decrease to 0.87 was evident for a ML of 25.2 % (HT_{wet} 170°C). This coincides with the many studies that show only a very limited effect of HT on the stiffness of wood [7,9,12,13]. The difference between HT_{dry} and HT_{wet} was very small with only a slight tendency to elevated MOE_{spec} ratios for HT_{dry} between 2 and 10 % ML.

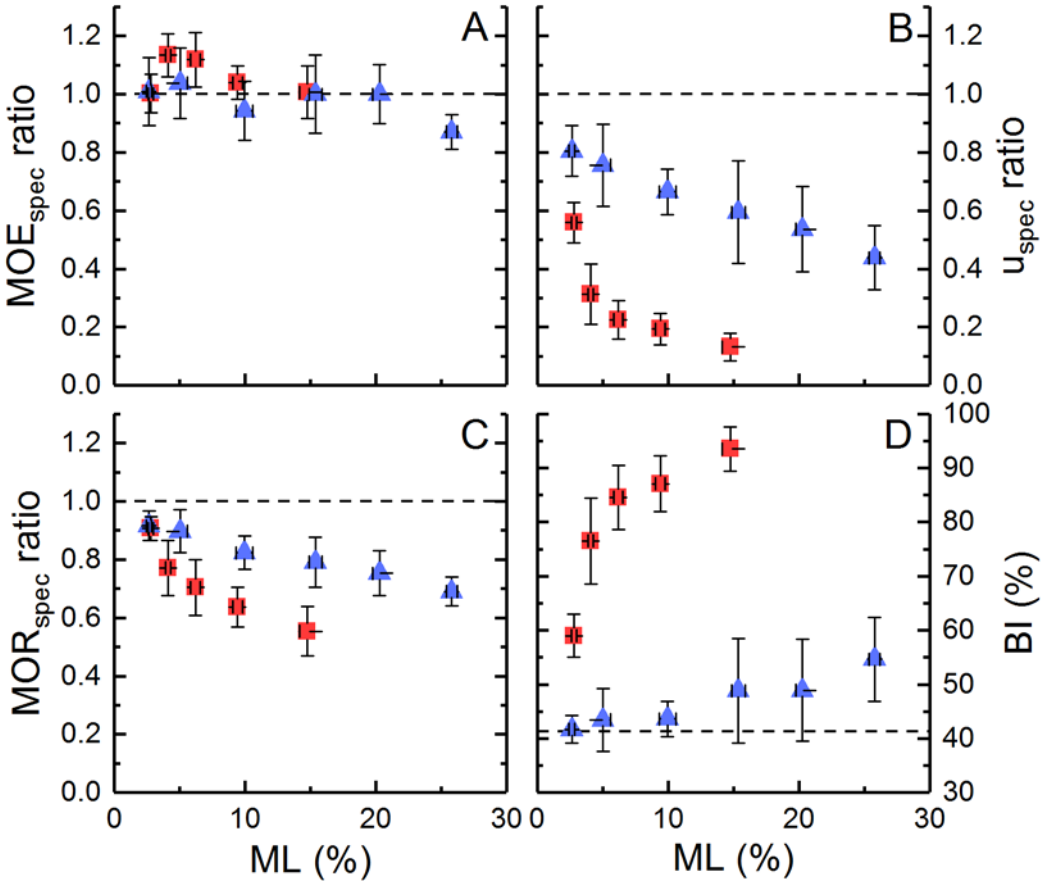

Figure 5: Bending properties given as ratios in dependence on the mass loss during the process (ML, %) for dry (squares) and wet (triangles) heat-treated Scots pine sapwood (N=15; ±95% confidence interval). A) MOE_{spec} ratio; B) u_{spec} ratio; C) MOR_{spec} ratio; D) BI (%). The dashed line highlights the average ratio of the reference samples.

In contrast to stiffness, MOR_{spec} and u_{spec} (**Figure 5** B and C) decreased as a function of ML, while the BI (**Figure 5** D) increased, in line with the de-polymerization sequence described by Winandy [8] and coinciding with previous studies [7,12,14]. However, there was a remarkable difference between the HT techniques applied, with a much stronger and non-linear change in MOR_{spec}, u_{spec} and BI as a function of ML for HT_{dry}. This difference was most pronounced for the BI and less noticeable in case of MOR_{spec}. The underestimation of hemicellulose de-polymerization by ML during HT_{dry} and overestimation during HT_{wet} cannot explain the differences between the HT techniques. As an example, the severest HT_{wet} resulted in a lower hemicellulose sugar ratio than the severest HT_{dry} (0.31 vs. 0.40), but in a higher MOR_{spec} ratio (0.69 vs. 0.55), a higher u_{spec} ratio (0.44 vs. 0.13) and a lower BI (55 % vs. 94 %). Cellulose degradation during HT_{dry} above 200 °C might have contributed to the change in mechanical behavior, but differences in u_{spec} and

brittleness index between HT_{dry} and HT_{wet} already occurred at ML levels below 5 %, at which no difference in the glucose ratio occurred. Thus, it is concluded that de-polymerization of cell wall constituents alone cannot explain the change in mechanical behavior during three-point bending of dry heat-treated wood.

Remarkably, HT_{dry} already lead to a BI above 80 % at ML levels below 10%, indicating that the maximum stress was reached with very little inelastic deformation (**Figure 5** D). At the same ML levels, no significant increase in BI was evident after HT_{wet}. The BI increased to a maximum of 55 % at higher ML levels for HT_{wet}, but the data scattering increased simultaneously. While there were individual samples that showed clear signs of embrittlement in their stress-strain curve, there were also wet heat-treated samples with a very ductile behavior and a BI well below the reference value. Interestingly, in the ML range between 14 and 20 %, some wet heat-treated samples, particularly those with MOR values above average, showed significant strain-softening effects during bending. This was observed as a monotonic decrease in stress as a function of strain after reaching a maximum, without any visible fracture. It indicates that the samples underwent considerable inelastic deformation before fracture, which is in clear contrast to the abrupt fracture after reaching maximum stress in dry heat-treated samples.

The differences in fracture modes of the dry and wet heat-treated samples, evident from bending test data, were also clearly visible during SEM observation of the fracture surfaces (tension side) of selected bending samples. Wood that was dry heat-treated at 240 °C displayed an almost flat fracture surface perpendicular to the grain (**Figure 6** A and B). In some regions, the fracture surface appeared almost as if cut with a blade without much signs of fibril-structures or other detachments remaining at the cell wall in axial orientation. Such a fracture is typical for the brittle failure of dry heat-treated wood sample tested in bending [58]. In contrast, wood that was wet heat-treated at 170 °C had a more ragged fracture surface with fibril structures being pulled out and sticking up from the cell walls (**Figure 6** C and D), thus resembling a typical fracture surface of a more ductile, unmodified wood sample [58]. This is especially remarkable, because the ML

and the loss in hemicellulose sugars recorded was higher for the wet heat-treated sample than for the dry heat-treated sample observed.

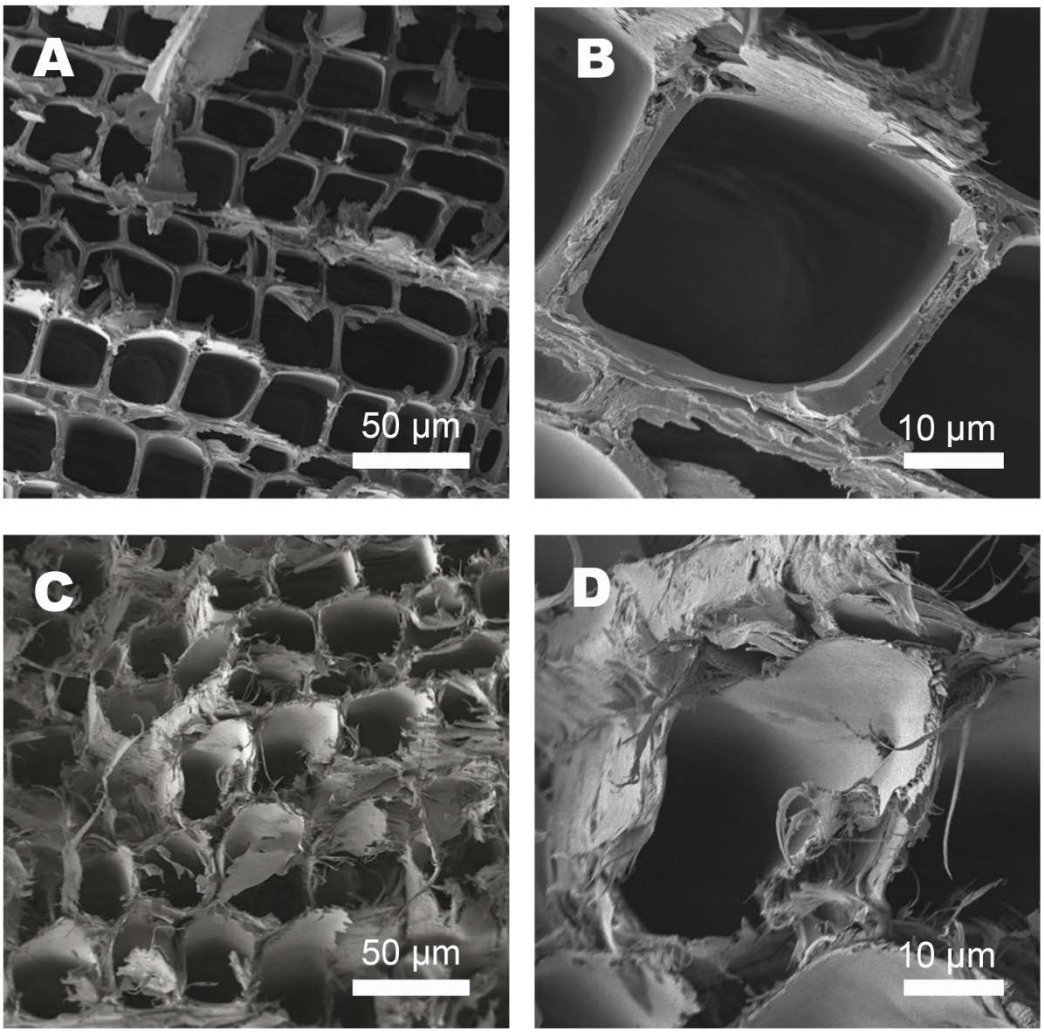

Figure 6: SEM images taken from the tension side of the fracture surface after the three-point bending test. The top row (A, B) shows a sample that was dry heat-treated at 240 °C; the bottom row (C, D) shows a sample that was wet heat-treated at 170 °C.

It may be argued that differences in the bending performance of the two HT techniques were caused by an increased formation of microscopic defects in dry heat-treated samples as a result of shrinkage stresses. Such defects could act as initials at which further crack propagation starts to cause a brittle failure during bending. However, drying was performed in the same way for all samples and no drying occurred during the actual HT processes. Shrinkage is also caused by the removal of cell wall polymers by degradation during HT [59], which causes stresses within the wood [60]. During HT_{dry}, degraded polymers were removed constantly as volatile compounds

[61], thus shrinkage stresses by polymer degradation built up gradually [60]. Such shrinkage occurred at elevated temperatures at which amorphous polymers are in a softened state [26,62], which eases stress relaxation. In contrast, water may act as spacer that prevents shrinkage during HT_{wet}, thus, shrinkage stresses by cell wall polymer removal occurred during final oven drying (40-103°C) after the process, when less cell wall polymers were in a softened state. Therefore, the formation of defects is more likely in wet heat-treated samples, which is in line with the observation of a high susceptibility to macroscopic crack formation in wet heat-treated wood during previous tests (unpublished results) and which renders a microscopic defect-cause unlikely.

Instead, we suggest that the differences in the bending behavior between the two HT techniques were predominantly caused by a mechanism that reduced inelastic deformation in dry heat-treated wood during bending. In theory, a decrease in inelastic deformation during bending would be most noticeable as a reduction in strain energy density and increase in brittleness index. The corresponding strength loss, however, would be less noticeable, because the increase in stress as a function of strain is comparably low in the inelastic region. This coincides with the differences in bending properties observed between HT_{dry} and HT_{wet}. Inelastic deformation involves the rearrangement of the cell wall polymers [63], which might be hindered by the formation of additional covalent bonds and cross-links in the cell wall matrix by re-polymerization reactions during HT_{dry}. The lack of inelastic deformation in dry heat-treated wood hinders the relaxation of stresses created by external loads, resulting in the built-up of high stress concentrations and a brittle failure of the material. Creation of additional covalent bonds within the cell wall matrix without de-polymerization of wood constituents by treatments of wood with cross-linking agents [64] or by incorporation of a rigid, three-dimensional corset of thermosetting resin such as melamine formaldehyde [65] result in a very similar change in mechanical performance during bending, i.e. in a significantly increased brittleness.

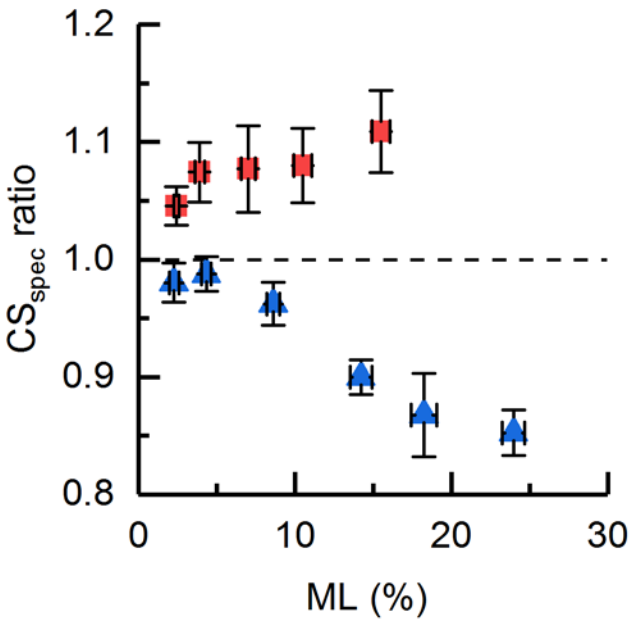

Figure 7: CS_{spec} (N=18) as a function of ML (%, N=6) for dry heat-treated (squares) and wet heat-treated (triangles) Scots pine sapwood. The dashed line highlights the reference value.

Inelastic deformation in unmodified wood during bending originates mostly from compression behavior during which the outer fibers at the top of the sample collapse or buckle [15]. On an ultra-structural level, the cellulose microfibrils buckle rapidly under compression loads parallel to the grain and rearrangements of the amorphous cell wall matrix polymers occur to cause inelastic deformation [20,21]. Therefore, the results of the compression test parallel to the grain (**Figure 7**), help in understanding the different failure modes of dry and wet heat-treated wood during bending. In case of HT_{dry}, additional covalent bond formation within the cell wall matrix enhanced the wood's resistance against compression loads, as evident from the increase in CS_{spec} as a function of ML. Since HT_{dry} is known to decrease the tensile strength to considerable extent [9], the increase in CS_{spec} resulted in a large decrease in the ratio of tensile to compression strength. Consequently, the failure in three-point bending of dry heat-treated wood was presumably caused by a brittle fracture in the tension zone with little or no inelastic deformation originating from compression at the top of the sample [15].

In contrast, CS_{spec} decreased after HT_{wet}, particularly beyond a ML level of 5 %. This is in line with preferential de-polymerization that results in fewer covalent bonds within the cell wall matrix

to resist compression loads. This loss in compression strength limited the decrease in the ratio of tensile to compression strength that would result from the loss in tensile strength caused by the de-polymerization of hemicelluloses in aqueous conditions [24]. Thus, bending failure was still accompanied by compression yielding after HT_{wet}, which resulted in only a slight increase in BI. In this context, strain-softening effects observed occasionally during bending of wet heat-treated wood can be interpreted as a distinct compression failure caused by an increase in the ratio of tensile to compression strength for a limited number of samples. This may also explain the high data scattering in the BI above 10 % ML caused by HT_{wet}.

4. Conclusions

The reduction in strength and strain energy density measured in three-point bending of wood that was wet heat-treated in pressurized hot water proceeded along the de-polymerization sequence reported previously. However, the mechanical behavior of wood that was dry heat-treated in superheated steam was additionally affected by the presence of additional covalent bonds and cross-links in the cell wall matrix as a result of re-polymerization reactions under dry heat conditions. Such bond formation hindered the inelastic deformation during bending of dry heat-treated wood to reduce strength, strain energy density and ductility to a much larger extent than observed for wet heat-treated wood. We suggest that the reduction in inelastic deformation in dry heat-treated wood originated mostly from an enhanced resistance against compression loads, which prevented compression yielding during bending and caused a brittle failure in tension. The results suggest the role of hemicellulose de-polymerization in causing a brittle behavior of the wood during bending to be much smaller than stated previously.

5. Acknowledgements

Financial support from the Academy of Finland (project number 309881) is acknowledged. Eero Stolt and Rita Hatakka are thanked for their assistance with the FT-IR spectroscopy and HPAEC-

PAD measurements. This work made use of the Aalto University Nanomicroscopy Center (Aalto-NMC) premises.

6. References

[1] Militz H, Altgen M. Processes and properties of thermally modified wood manufactured in Europe. In: Schultz TP, Goodell B, Nicholas DD, editors. Deterioration and protection of sustainable biomaterials, American Chemical Society, 2014: ACS Symposium Series 1158, Chapter 16, pp. 269–285.

[2] Scheiding W. TMT in the year 2016 – an update. Proceedings of the 9th European TMT-Workshop, Dresden, Germany, 2016, pp. 12-18.

[3] Stamm AJ, Hansen LA. Minimizing wood shrinkage and swelling effect of heating in various gases. Ind Eng Chem 1937;29(7):831–833. doi:10.1021/ie50331a021.

[4] Kamdem DP, Pizzi A, Jermannaud A. Durability of heat-treated wood. Eur J Wood Wood Prod (2002);60(1):1–6. doi:10.1007/s00107-001-0261-1.

[5] Hakkou M, Pétrissans M, Gérardin P, Zoulalian A. Investigations of the reasons for fungal durability of heat-treated beech wood. Polym Degrad Stab (2006);91(2):393–397. doi:10.1016/j.polymdegradstab.2004.04.042.

[6] Hughes M, Hill C, Pfriem A, The toughness of hygrothermally modified wood - a review. Holzforschung (2015);69(7): 851-862. doi:10.1515/hf-2014-0184.

[7] Kubojima Y, Okano T, Ohta M. Bending strength and toughness of heat-treated wood. J Wood Sci (2000);46(1):8–15. doi:10.1007/bf00779547.

[8] Winandy JE. Relating wood chemistry and strength: Part II. Fundamental relationships between changes in wood chemistry and strength of wood. Wood Fiber Sci (2017);49(1):1–10.

[9] Boonstra MJ, Van Acker J, Tjeerdsma BF, Kegel EV. Strength properties of thermally modified softwoods and its relation to polymeric structural wood constituents. Ann For Sci (2007);64(7):679–690. doi:10.1051/forest:2007048.

[10] LeVan SM, Ross RJ, Winandy JE. Effects of fire retardant chemicals on the bending properties of wood at elevated temperatures. USDA Res. Pap. FPL-PR-498 Madison WI. (1990).

[11] Winandy JE, Krzysik AM. Thermal degradation of wood fibers during hot-pressing of MDF composites: Part I. Relative effects and benefits of thermal exposure. Wood Fiber Sci (2007);39(3):450–461.

[12] Borrega M, Kärenlampi PP. Mechanical behavior of heat-treated spruce (*Picea abies*) wood at constant moisture content and ambient humidity. Holz als Roh- Werkst (2008);66(1):63–69.

[13] Altgen M, Militz H. Influence of process conditions on hygroscopicity and mechanical properties of thermally modified wood in a closed reactor system. Holzforschung (2016);70(10):971–979.

[14] Phuong L, Shida S, Saito Y. Effects of heat treatment on brittleness of *Styrax tonkinensis* wood. J Wood Sci (2007);53(3):181–186. doi:10.1007/s10086-006-0841-0.

[15] Buchanan AH. Bending strength of lumber. J Struct Eng (1990);116(5):1213–1229. doi:10.1061/(ASCE)0733-9445(1990)116:5(1213).

[16] Burgert I. Exploring the micromechanical design of plant cell walls. Am. J. Bot. 93 (2006) 1391–1401. doi:10.3732/ajb.93.10.1391.

[17] Salmén L, Burgert I. Cell wall features with regard to mechanical performance. A review COST Action E35 2004–2008: Wood machining - micromechanics and fracture. Holzforschung (2009);63(2):121-129. doi:10.1515/hf.2009.011.

[18] Stevanic JS, Salmén L. Orientation of the wood polymers in the cell wall of spruce wood fibres. Holzforschung (2009);63(3):497-503. doi:10.1515/hf.2009.094.
[19] Eichhorn SJ, Young RJ. The Young's modulus of a microcrystalline cellulose. Cellulose (2001);8(3):197–207. doi:10.1023/A:1013181804540.
[20] Gindl W, Gupta HS, Schöberl T, Lichtenegger HC, Fratzl P. Mechanical properties of spruce wood cell walls by nanoindentation. Appl Phys A (2004);79(8):2069–2073. doi:10.1007/s00339-004-2864-y.
[21] Gindl W, Teischinger A. Axial compression strength of Norway spruce related to structural variability and lignin content. Compos Part Appl Sci Manuf (2002);33(12): 1623–1628. doi:10.1016/S1359-835X(02)00182-3.
[22] Gindl W. Comparing mechanical properties of normal and compression wood in Norway spruce: The role of lignin in compression parallel to the grain. Holzforschung (2002);56(4):395–401.
[23] Lagergren S, Rydholm S, Stockman L. Studies on the interfibre bonds of wood. Part 1: Tensile strength of wood after heating, swelling and delignification. Sven Papperstidn (1957);60:632–644 60 (1957) 632–644.
[24] Klüppel A, Mai C. Effect of lignin and hemicelluloses on the tensile strength of micro-veneers determined at finite span and zero span. Holzforschung (2012);66(4):493–496. doi:10.1515/hf.2011.173.
[25] Whistler RL, Chen CC. Hemicelluloses, In: Lewin M, Goldstein IS, editors. Wood structure and composition, Marcel Decker, Inc., New York, 1991, Chapter 7, pp.287-319.
[26] Salmén L, Olsson AM. Interaction between hemicelluloses, lignin and cellulose: Structure-property relationships. J Pulp Pap Sci (1998);24(3):99–103.
[27] Kollmann F, Fengel D. Änderungen der chemischen Zusammensetzung von Holz durch thermische Behandlung. Holz als Roh- Werkst (1965);23(12):461–468. doi:10.1007/bf02627217.
[28] Kotilainen R. Chemical changes in wood during heating at 150-260°C. Doctoral thesis, University of Jyväskylä, Finland, 2000.
[29] Karlsson O, Torniainen P, Dagbro O, Granlund K, Morén T, Presence of water-soluble compounds in thermally modified wood: Carbohydrates and furfural. BioResources (2012);7(3):3679–3689.
[30] Alén R, Kotilainen R, Zaman A. Thermochemical behavior of Norway spruce (*Picea abies*) at 180-225 degrees C. Wood Sci Technol (2002);362):163–171. doi:10.1007/s00226-001-0133-1.
[31] Esteves B, Marques AV, Domingos I, Pereira H. Influence of steam heating on the properties of pine (*Pinus pinaster*) and eucalypt (*Eucalyptus globulus*) wood. Wood Sci Technol (2007);41:193–207. doi:10.1007/s00226-006-0099-0.
[32] Welzbacher CR, Rassam G, Talaei A, Brischke C. Microstructure, strength and structural integrity of heat-treated beech and spruce wood. Wood Mater Sci Eng (2011);6(4):219–227. doi:10.1080/17480272.2011.622411.
[33] Tjeerdsma BF, Boonstra M, Pizzi A, Tekely P, Militz H. Characterisation of thermally modified wood: molecular reasons for wood performance improvement. Holz als Roh-Werkst (1998);56(3):149–153.
[34] Tjeerdsma BF, Militz H. Chemical changes in hydrothermal treated wood: FTIR analysis of combined hydrothermal and dry heat-treated wood. Holz als Roh- Werkst (2005);63(2):102–111. doi:10.1007/s00107-004-0532-8.
[35] Liang T, Wang L. Thermal treatment of poplar hemicelluloses at 180 to 220 °C under nitrogen atmosphere. BioResources (2017);12(1):1128–1135.
[36] Inari GN, Mounguengui S, Dumarçay S, Pétrissans M, Gérardin P. Evidence of char formation during wood heat treatment by mild pyrolysis. Polym Degrad Stab (2007);92(6):997–1002. doi:http://dx.doi.org/10.1016/j.polymdegradstab.2007.03.003.

[37] Brosse N, El Hage R, Chaouch M, Pétrissans M, Dumarcay S, Gérardin P. Investigation of the chemical modifications of beech wood lignin during heat treatment. Polym Degrad Stab (2010);95(9):1721–1726. doi:10.1016/j.polymdegradstab.2010.05.018.
[38] Engelund Thybring E, Thygesen LG, Burgert I. Hydroxyl accessibility in wood cell walls as affected by drying and re-wetting procedures. Cellulose (2017);24(6): 2375-2384. doi:10.1007/s10570-017-1278-x.
[39] Sluiter A, Hames B, Ruiz R, Scarlata C, Sluiter J, Templeton D, Crocker D. Determination of structural carbohydrates and lignin in biomass. National Renewable Energy Laboratory (NREL), USA, 2012, Technical report NREL/TP-510-42618.
[40] Zou X, Gurnagul N, Uesaka T, Bouchard J. Accelerated aging of papers of pure cellulose: mechanism of cellulose degradation and paper embrittlement. Polym Degrad Stab (1994);43(3):393–402. doi:10.1016/0141-3910(94)90011-6.
[41] Garrote G, Domínguez H, Parajó JC. Hydrothermal processing of lignocellulosic materials. Holz als Roh- Werkst (1999);57(3):191–202. doi:10.1007/s001070050039.
[42] Garrote G, Domínguez H, Parajó JC. Study on the deacetylation of hemicelluloses during the hydrothermal processing of Eucalyptus wood. Holz als Roh- Werkst (2001);59(1-2):53–59. doi:10.1007/s001070050473.
[43] Li J, Henriksson G, Gellerstedt G. Lignin depolymerization/repolymerization and its critical role for delignification of aspen wood by steam explosion. Bioresour Technol (2007);98(16):3061–3068. doi:10.1016/j.biortech.2006.10.018.
[44] Borrega M, Nieminen K, Sixta H. Effects of hot water extraction in a batch reactor on delignification of birch wood. BioResources (2011); 6(2):1890–1903.
[45] Binder JB, Raines RT. Fermentable sugars by chemical hydrolysis of biomass. Proc Natl Acad Sci (2010);107(10):4516–4521. doi:10.1073/pnas.0912073107.
[46] Dee SJ, Bell AT. A study of the acid-catalyzed hydrolysis of cellulose dissolved in ionic liquids and the factors influencing the dehydration of glucose and the formation of humins. ChemSusChem (2011);4(8):1166–1173. doi:10.1002/cssc.201000426.
[47] Enslow KR, Bell AT. The kinetics of Brønsted acid-catalyzed hydrolysis of hemicellulose dissolved in 1-ethyl-3-methylimidazolium chloride, RSC Adv (2012);2(26):10028–10036. doi:10.1039/C2RA21650G.
[48] Runkel RH, Lüthgens M. Untersuchungen über die Heterogenität der Wassersorption der chemischen und morphologischen Komponenten verholzter Zellwände. Holz als Roh-Werkst (1956);14(11):424–441. doi:10.1007/bf02614975.
[49] Fengel D. On the changes of the wood and its components within the temperature range up to 200°C—Part IV: The behaviour of cellulose in spruce wood under thermal treatment. Holz als Roh- Werkst (1967);25(3):102–111. doi:10.1007/BF02608251.
[50] Emsley AM, Stevens GC. Kinetics and mechanisms of the low-temperature degradation of cellulose. Cellulose (1994);1(1):26–56. doi:10.1007/bf00818797.
[51] Faix O. Classification of lignins from different botanical origins by FT-IR spectroscopy. Holzforschung (1991);45(s1):21-27. doi:10.1515/hfsg.1991.45.s1.21.
[52] Windeisen E, Strobel C, Wegener G. Chemical changes during the production of thermo-treated beech wood. Wood Sci Technol (2007);41(6):523–536. doi:10.1007/s00226-007-0146-5.
[53] Chow SZ. Infrared spectral characteristics and surface inactivation of wood at high temperatures. Wood Sci Technol (1971);5(1):27–39. doi:10.1007/bf00363118.
[54] Kotilainen RA, Toivanen TJ, Alén RJ. FTIR monitoring of chemical changes in softwood during heating. J Wood Chem Technol (2000);20(3):307–320.
[55] Li J, Li B, Zhang X. Comparative studies of thermal degradation between larch lignin and manchurian ash lignin. Polym Degrad Stab (2002);78(2):279–285. doi:10.1016/S0141-3910(02)00172-6.
[56] Kocaefe D, Poncsak S, Boluk Y. Effect of thermal treatment on the chemical composition and mechanical properties of birch and aspen. Bioresources (2008);3(2):517–537.

[57] González-Peña MM, Hale MDC. Colour in thermally modified wood of beech, Norway spruce and Scots pine. Part 1: Colour evolution and colour changes. Holzforschung (2009);63(4):385–393. doi:10.1515/hf.2009.078.
[58] Boonstra M, Rijsdijk JF, Sander C, Kegel E, Tjeerdsma B, Militz M, Van Acker J, Stevens M. Microstructural and physical aspects of heat treated wood. Part 1: Softwoods. Maderas Cienc Tecnol (2006);8(3):193–208.
[59] González-Peña MM, Curling SF, Hale MDC. On the effect of heat on the chemical composition and dimensions of thermally-modified wood. Polym Degrad Stab (2009);94(12):2184–2193. doi:10.1016/j.polymdegradstab.2009.09.003.
[60] Cheng W, Morooka T, Wu Q, Liu Y. Characterization of tangential shrinkage stresses of wood during drying under superheated steam above 100°C. For Prod J (2007);57(11):39–43.
[61] Welzbacher CR, Brischke C. Interrelationship between heat treatment intensity and gas emissions as a tool for the dynamic process control, In: Jones D, Militz H, Petrič M, Pohleven F, Humar M, Pavlič M, editors. Proceedings of the 6th European Conference on Wood Modification (ECWM), Ljubljana, Slovenia, 2012, pp. 539–547.
[62] Chow SZ, Pickles KJ. Thermal softening and degradation of wood and bark. Wood Fiber Sci (1971);3(3):66–178.
[63] Winandy JE, Rowell RM. Chemistry of wood strength, In: Rowell RM, editor. Handbook of Wood Chemistry and Wood Composites., CRC Press, 2005, Chapter 11, pp. 303-347.
[64] Burmester A. Versuche zur Behandlung von Holz mit monomeren Formaldehyd-Gas unter Verwendung von Gamma-Strahlen. Holzforschung (1967);21(1):13–20.
[65] Pittman CU, Kim MG, Nicholas DD, Wang L, Kabir FRA, Schultz TP, Ingram LL. Wood enhancement treatments I. Impregnation of southern yellow pine with melamine-formaldehyde and melamine-ammeline-formaldehyde resins, J Wood Chem Technol (1994);14(4):577–603. doi:10.1080/02773819408003114.